An occurrence of similar to 74 ka Youngest Toba Tephra from the Western Continental Margin of India

Pattan, JN; Shane, P; Pearce, NJG; Banakar, VK; Parthiban, G

Published in:
Current Science

Publication date:
2001

Citation for published version (APA):
Pattan, JN., Shane, P., Pearce, NJG., Banakar, VK., & Parthiban, G. (2001). An occurrence of similar to 74 ka Youngest Toba Tephra from the Western Continental Margin of India. *Current Science*, *80*(10), 1322-1326. http://hdl.handle.net/2160/7217

(D in Figure 1 *a*). It is interesting to note that some of the features, which are reflected very well in the T_b maps of July and August are not seen so well in the T_b map for the last week of October (Figure 1 *c*). This could be attributed to the fact that the contrast in the T_b between two different elevations reduces with the increasing physical temperatures in Antarctica due to the onset of summer in the month of October.

The above study demonstrates the capability of MSMR on-board OCEANSAT-1 in capturing the sea-ice distribution over the Antarctic Circumpolar Sea, as well as the land-ice signatures matching with some known geomorphological features on the continent of Antarctica, thus giving confidence in using MSMR data for studies of earth's polar regions. Quantitative estimation of sea-ice concentration and studies of sea-ice distribution and dynamics are being attempted separately with the help of multi-channel MSMR observations and will be reported soon. Availability of 6.6/10.65 GHz channels on MSMR, not existing on SSM/I, in Antarctic ice studies is also being explored.

1. Gloersen, P., Nordberg, W., Schmugge, T. J., Wilheit, T. T. and Campbell, W. J., *J. Geophys. Res*., 1973, **78**, 3564–3572.
2. Gloersen, P., Campbell, W. J., Cavalier, D. J., Comiso, J. C., Parkinson, C. L. and Zwally, H. J., Report, NASA SP–511, 1992, pp. 1–290.
3. Steffen, K. and Schweiger, A., *J. Geophys. Res*., 1991, **96**, 21971–21987.
4. Majumdar, T. J. and Mohanty, K. K., *Curr. Sci*., 2000, **79**, 648–651.
5. Brigham, A. W. and Drinkwater, M. R., *IEEE GS&RS*, 2000, **38**, 1810–1816.
6. Report, Indian Space Research Organization, 1999, pp. 1–7.
7. Fu, C. C., Han, D., Kim, S. T. and Gloersen, P., Report, NASA RP-1210, 1988, p. 158.

ACKNOWLEDGEMENTS. We wish to acknowledge the encouragement given by Dr R. R. Navalgund and Dr M. S. Narayanan during the course of this work. Useful discussions with Dr P. S. Desai and Dr A. Sarkar are also thankfully acknowledged.

Received 28 July 2000; revised accepted 3 January 2001

An occurrence of ~ 74 ka Youngest Toba Tephra from the Western Continental Margin of India

J. N. Pattan[†,*], P. Shane[#], N. J. G. Pearce[‡], V. K. Banakar[†] and G. Parthiban[†]

[†]National Institute of Oceanography, Dona Paula, Goa 403 004, India
[#]Department of Geology, University of Auckland, P.B. 92019, Auckland, New Zealand
[‡]Institute of Geography and Earth Sciences, University of Wales, Aberystwyth, SY23 3DB, UK

A dispersed volcanic ash layer was recovered at ~ 300 cm depth in a 5.52 m long sediment core collected at a latitude 9°21′N and longitude 71°59′E from a water depth of 2300 m on the Western Continental Margin of India (WCMI). Glass shards from ash layer were studied for morphology, major, trace and rare earth element concentration to trace the source. Bubble wall junction-type morphology of glass shard suggests magmatic origin. Shards have high SiO_2 (77%) and total alkalis (8.5%), indicating rhyolitic composition. The major, trace and rare earth element composition of these glass shards are indistinguishable from that of Youngest Toba ash of ~ 74 ka from the Northern Sumatra and confirm as the source. The new occurrence of Youngest Toba Tuff from the WCMI, Central Indian Ocean Basin and South China Sea Basin suggests a reassessment of the ash volume and global climatic implications.

VOLCANIC ash in marine sediments is derived either from the continent through wind and river runoff or from *in situ* submarine volcanism. Ash layers of variable thickness in the Bay of Bengal, north-eastern Indian Ocean, Indian subcontinent and Central Indian Ocean Basin were noticed and were attributed to different sources[1–10]. During International Indian Ocean Expedition (1960–1965), a number of sediment cores were retrieved along the Western Continental Margin of India (WCMI). Some sediment cores contained dispersed volcanic glass shards at subsurface depths, but their origin could not be traced[11]. Recently, we have recovered a dispersed ash layer ~ 34 cm thick (324–290 cm depth) in one of the cores collected from the WCMI. The present study is made on this ash to trace the source.

A 5.52 m long sediment core was raised from a water depth of 2300 m at a latitude 9°21′N and longitude 71°59′E from the WCMI in the Arabian Sea, using a gravity corer during ORV *Sagar Kanya* cruise 129 (Figure 1). The core was subsampled at 2 cm intervals onboard and in the laboratory sediment was made salt-free and the coarse fraction (> 63 μm) was obtained by wet sieving. Abundant volcanic glass shards were found between 324 and 290 cm interval of the coarse fraction. The glass shards were separated using heavy liquid bromoform and cleaned ultrasonically. Morphology of glass shards was studied using scanning electron microscopy (JSM-5800LV). Purified glass shards were mounted in epoxy resin and polished to expose internal features. Major element oxides were analysed using Jeol JXA-5A electron microprobe fitted with a Link Systems LZ-5 EDS detector with an absorbed current of 0.5 nA at 15 kV and a beam focused at 10 μm. Thirteen trace and fourteen naturally occurring rare earth elements (REE) were determined for these glass shards using a VG Elemental Plasma Quad II + Inductively Coupled Plasma-Mass Spectrometry (ICP-MS)

*For correspondence. (e-mail: pattan@csnio.ren.nic.in)

with a modified high-sensitivity interface, using fully quantitative solution analysis method as described earlier[5,12].

The glass shards appear fresh with different sizes and shapes, are shining, colourless, isotropic and exhibit no signs of alteration. Most of the shards are of bubble wall junction-type with cuspate and flat morphology (Figure 2 *a* and *b*). Shards with Y-shaped wall fragments suggest that the shape is the remnant of three connected bubbles (Figure 2 *c*). Pumice fragments have elongated cellular vesicles (Figure 2 *d*). These morphological features suggest that these shards are of magmatic type[13] and preclude the possibility of *in situ* origin. Shards with a similar morphology from the Indian subcontinent have been noticed recently[14]. Abundant pyrite framboids are found within this 34-cm ash layer. When glass shards fall on the sea surface and sink through the water column, organic matter may adhere to the glass shard, resulting in the deposition of higher levels of organic matter on the sea-floor. The oxidation of this organic matter may result in H_2S formation and in turn reaction with iron may produce abundant pyrite framboids (Figure 2 *e* and *f*). The presence of framboidal pyrite in the marine environment suggests either diagenetic sulphate reduction or euxinic bottom waters[15]. The EDAX analysis of these pyrite grains showed high Fe_2O_3 (38%) and SO_3 (55%), and low SiO_2 (3.3%).

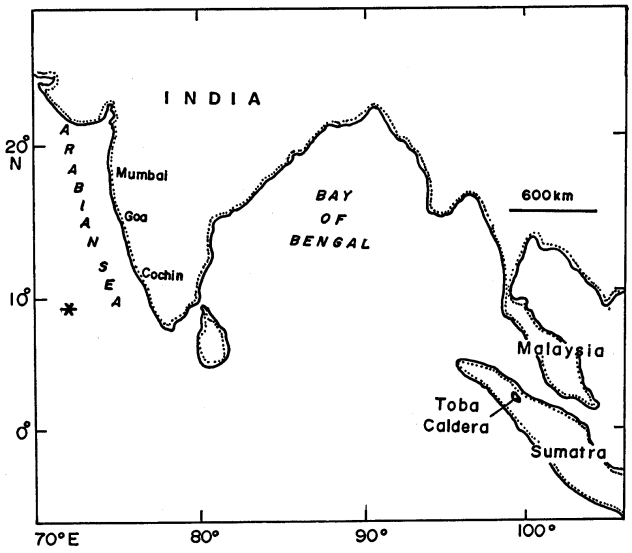

Figure 1. Map showing location of sediment core (*) in which ash layer was found at 324–290 cm interval.

The chemical composition of glass shards is dominated by silica (77%) and alkalis (8.5%), with minor amounts of FeO (0.88%), CaO (0.83%), TiO_2 (0.12%) and MnO (0.12%) (Table 1). The total alkalis and silica content indicates a rhyolitic composition. The similar major element composition of glass shards from 320 to 322 cm and 290 to 292 cm depth intervals suggests a

Table 1. Electron microprobe data (%) of glass shards from the Western Continental Margin of India

	SiO_2	Al_2O_3	TiO_2	FeO	MnO	MgO	CaO	Na_2O	K_2O	Cl	H_2O
Depth											
290–292 nm											
	76.95	12.45	0.10	0.88	0.06	–	0.68	3.61	5.15	0.13	5.55
	76.92	12.66	0.04	0.85	0.12	–	0.89	3.23	5.16	0.13	5.99
	77.05	12.62	0.15	0.96	0.00	–	0.98	3.43	4.71	0.11	6.89
	77.12	12.41	0.16	0.85	0.05	–	0.90	3.26	5.13	0.12	6.22
	77.24	12.34	0.05	0.87	0.14	–	0.63	3.48	5.13	0.13	5.90
	77.05	12.50	0.10	0.88	0.07	–	0.81	3.40	5.06	0.12	6.11
320–322 cm											
	77.44	12.40	0.05	0.69	0.13	–	0.83	3.47	4.88	0.11	7.31
	76.77	12.67	0.11	0.96	0.16	–	0.94	3.25	5.09	0.05	6.44
	76.55	12.71	0.20	0.96	0.02	–	0.91	3.40	5.15	0.10	5.43
	76.82	12.46	0.18	0.95	0.08	–	0.80	3.51	5.05	0.14	5.47
	76.93	12.64	0.17	0.85	0.10	–	0.76	3.38	5.03	0.14	5.65
	76.90	12.58	0.14	0.88	0.10	–	0.85	3.40	5.04	0.11	6.06
Mean	76.94	12.53	0.12	0.88	0.12	–	0.83	3.40	5.04	0.12	6.08
	(0.33)	(0.14)	(0.06)	(0.12)	(0.05)	–	(0.15)	(0.16)	(0.19)	(0.03)	(0.81)
Westgate *et al.*[5]	77.58	12.60	0.06	0.90	0.06	0.05	0.77	3.24	4.96	0.14	1.99
(n = 275)	(0.23)	(0.13)	(0.04)	(0.05)	(0.03)	(0.02)	(0.07)	(0.13)	(0.14)	(0.03)	(0.83)
Pattan *et al.*[6]	76.81	12.77	0.07	0.92	0.06	0.05	0.79	3.41	5.08	0.16	5.23
(n = 91)	(0.22)	(0.12)	(0.04)	(0.07)	(0.04)	(0.03)	(0.07)	(0.13)	(0.16)	(0.03)	(0.97)

Analytical data are recalculated to 100% on a volatile free basis; H_2O is by difference; Total Fe as FeO; Values in the bracket are standard deviation; –, Below detection.

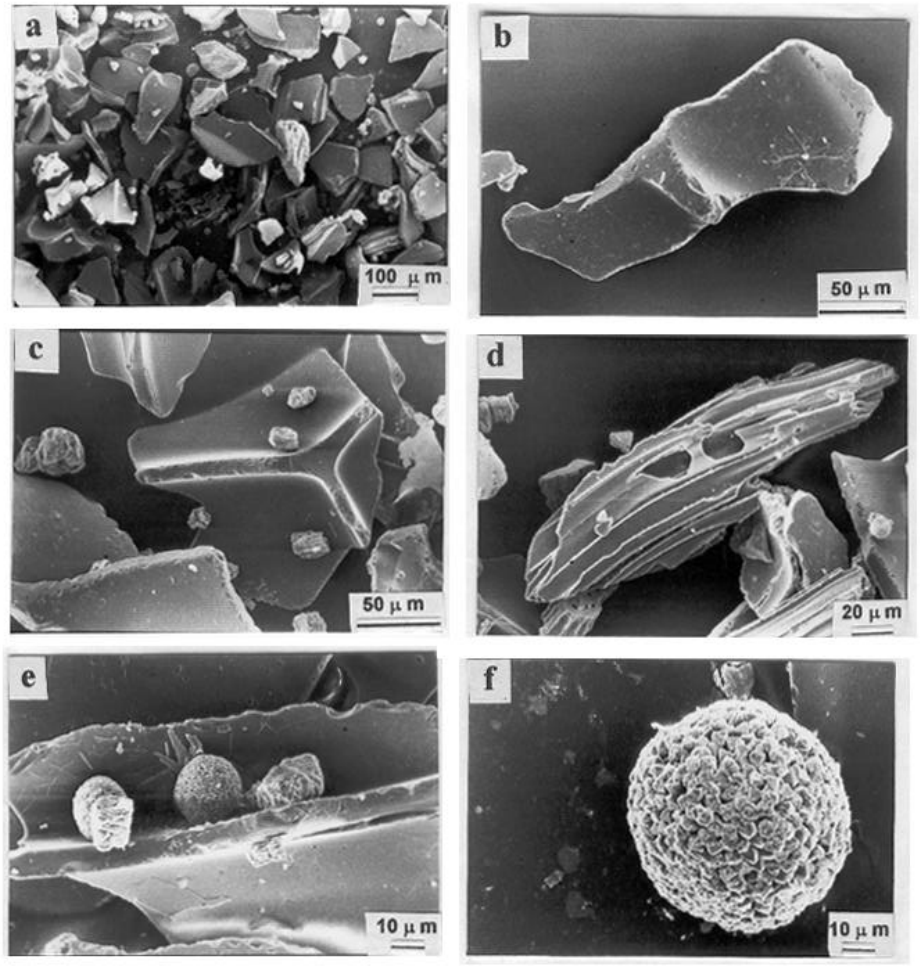

Figure 2. Scanning electron microphotographs of glass shards. ***a***, Glass shards of different sizes and shapes; ***b***, Flat morphology like a human leg and a radial crack in the upper part of shard which could be due to aerodynamics during its journey; ***c***, Y-shaped glass shard formed between three bubbles; ***d***, Pumice shard with parallel vesicles; ***e***, Pyrite framboid sitting on glass shard; and ***f***, Enlarged individual pyrite framboid.

sediment reworking (Table 1). The plot of CaO vs FeO for the WCMI glass shards falls within the area that characterizes the Youngest Toba ash (Figure 3)[5,6,16]. The ∑REE concentration of the glass shards varies from 120 to 166 ppm with an average of 139 ppm (Table 2). The chondrite-normalized REE patterns for the WCMI shards exhibit light REE (LREE) enrichment over heavy REE (HREE), with a strong negative Eu-anomaly (Figure 3). The major and trace element concentration and their ratios (La/Lu, Zr/Hf, Nb/Ta, Zr/Nb, Cs/Yb, Ce/Y and Th/U), REE concentration and chondrite-normalized REE pattern of glass shards are very similar to the Youngest Toba ash of ~ 74 ka from Northern Sumatra[5] and confirm their source. This is the first report on the occurrence of Youngest Toba ash from the WCMI. Its occurrence in other parts of the earth should be looked into. Recently, Song *et al.*[17] further traced Youngest Toba Tuff (YTT) in the South China Sea Basin which is 1500 km NE of Toba cladera, which is further widening its aerial extension. Volcanic ash was used to trace the palaeowind direction. The occurrence of YTT in the west, north-west, south-west and recently north-east in the South China Sea Basin[17], suggests wind direction during YTT was not in one way.

YTT occurred between oxygen isotope stage 5a and 4, a period of ice growth and falling global sea level[18]. The volcanic aerosols and fine ash dust from YTT were injected into the stratosphere and might have accelerated the global cooling process. The new occurrence of YTT from WCMI, Central Indian Ocean Basin and South China Sea Basin suggests that the ash volume and climatic implications were underestimated and reassessment is needed.

The Toba caldera from the Northern Sumatra erupted in the past at ~ 74 ka, ~ 540 ka and ~ 840 ka known as Youngest Toba Tuff (YTT), Middle Toba Tuff (MTT)

Table 2. Trace and rare earth element concentration (ppm) of glass shards from the Western Continental Margin of India

Element	Isotope used	WCMI-1 290–300 cm	WCMI-2 300–310 cm	WCMI-3 310–324 cm	Mean	Westgate *et al.*[5]	Pattan *et al.* unpublished
Be	9	2.94	2.59	3.54	3.02	–	2.42
Ti	49	680	490	598	589	–	548
Rb	85	225	236	274	245	222	211
Sr	88	64.9	58.4	75.3	66.2	42.5	53.6
Y	89	33.2	30.9	45.2	34.5	30.7	26.9
Zr	90	79.7	82.1	97.9	86.7	76.2	73.9
Nb	93	14.5	15.5	16.1	15.4	13.0	13.0
Cs	133	9.1	8.6	10.2	9.3	7.6	9.1
Ba	138	461	438	530	476	348	425
La	139	30.2	27.9	38.3	32.1	29.9	27.2
Ce	140	50.5	46.1	61.2	52.6	48.6	50.2
Pr	141	6.2	5.6	7.9	6.6	5.4	5.4
Nd	146	19.6	17.6	25.4	20.9	19.1	18.6
Sm	147	4.5	3.9	5.6	4.7	4.1	3.92
Eu	151	0.61	0.51	0.83	0.65	0.40	0.50
Gd	157	4.66	4.21	6.60	5.15	4.29	4.11
Tb	159	0.76	0.74	1.06	0.85	0.73	0.70
Dy	162	5.31	4.71	7.11	5.71	4.81	4.47
Ho	165	1.06	0.98	1.44	1.16	1.04	0.95
Er	166	3.23	2.92	4.26	3.47	3.18	3.03
Tm	169	0.77	0.64	0.92	0.77	0.53	0.63
Yb	174	3.76	3.46	4.83	4.01	3.70	3.85
Lu	175	0.84	0.70	1.06	0.86	0.60	0.64
Hf	178	3.43	3.35	3.70	3.49	3.15	3.15
Ta	181	1.24	2.06	1.08	1.46	1.30	1.45
Pb	208	34.1	33.9	38.9	35.7	–	–
Th	232	31.9	31.3	35.9	33.1	28.1	26.71
U	238	5.93	5.43	6.48	5.94	5.07	6.98

Westgate *et al.*[5], Mean of 15 glass shards of Youngest Toba origin from Malaysia, Sumatra, India, and Bay of Bengal; Pattan *et al.* (unpublished), Mean of 8 glass shards of Youngest Toba origin form Central Indian Ocean Basin; –, Not analysed.

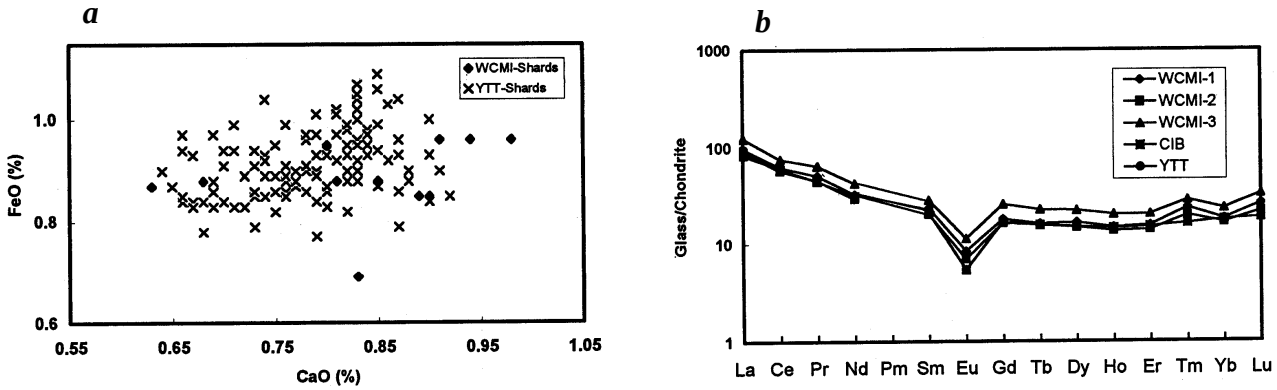

Figure 3. ***a***, Plot of CaO (%) vs FeO (%) for the glass shards from WCMI (◆) and from Youngest Toba ash of 74 ka (×); ***b***, Chondrite-normalized REE pattern of purified glass from the WCMI and those reported earlier for Youngest Toba ash of ~74 ka.

and Oldest Toba Tuff (OTT), respectively[19]. The glass shards from the WCMI are further distinguished by MTT and OTT, with high concentration of K, Rb, Cs, Th, U, Ta, Y and heavy REE and low concentration of Fe, Na and light REE, whereas Ca, Mn, Mg, Sr, Ba, Zr and Cl have intermediate composition between MTT and OTT[5].

Morphology, major, trace and REE concentration of shards from the WCMI suggest Youngest Toba ash (~74 ka) from the Northern Sumatra as the source. The aerial extension of Youngest Toba ash in other parts of the earth should be looked into and ash volume and climatic impact should be reassessed.

1. Ninkovich, D., Shackleton, N. J., Abdel-Monem, A. A., Obradovich, J. D. and Izett, G., *Nature*, 1978, **276**, 574–577.
2. Rose, W. I. and Chesner, C. A., *Geology*, 1987, **15**, 913–917.
3. Dehn, J., Farrel, J. W. and Schmincke, H. U., Proceedings of the ODP, Scientific Results, 1991, vol. 121, pp. 273–295.

4. Gupta, S. M., *J. Palaeontol. Soc. India*, 1988, **33**, 59–71.
5. Westgate, J. A. *et al.*, *Quat. Res.*, 1998, **50**, 107–112.
6. Pattan, J. N., Shane, P. and Banakar, V. K., *Mar. Geol.*, 1999, **155**, 243–248.
7. Williams, M. A. J. and Royce, K., *Palaeogeogr. Palaeoclimatol. Palaeoecol.*, 1982, **38**, 139–162.
8. Basu, P. K., Biswas, S. and Acharyya, S. K., *Indian Miner.*, 1987, **41**, 66–72.
9. Korisettar, R. *et al.*, *Curr. Sci.*, 1989, **58**, 564–567.
10. Acharyya, S. K. and Basu, P. K., *Quat. Res.*, 1993, **40**, 10–19.
11. Stackelberg, V. U., Faziesverteiling in sedimenten des Indisch-Pakistanischen Kontinentalran des Metero – Forschungsergebnisse, 1972, Reiche C-No 9, 1–73.
12. Pearce, N. J. G., Perkins, W. T., Westgate, J. A., Gorton, M. P., Jackson, S. E., Neal, C. R. and Chenery, S. P., *Geostand. Newsl.*, 1997, **21**, 115–144.
13. Heiken, G., *Geol. Soc. Am. Bull.*, 1972, **83**, 1962–1988.
14. Karmalkar, N. R., Ghate, S. N., Mishra, S. and Rajguru, S. N., *J. Geol. Soc. India*, 1998, **51**, 213–218.
15. Masuzawa, T., Takada, J. and Matsushita, Proceedings of ODP, Scientific Results, 1992, vol. 127/128, pp. 705–717.
16. Shane, P., Westgate, J., Williams, J. and Korishettar, R., *Quat. Res.*, 1995, **44**, 200–204.
17. Song, S. R., Chen, C. H., Lee, M. Y., Yang, T. F., Iizuka, Y. and Wei, K. Y., *Mar. Geol.*, 2000, **167**, 303–312.
18. Rampino, M. R. and Self, S., *Quat. Res.*, 1993, **40**, 269–280.
19. Chesner, C. A., Ph D thesis, Michigan Technology University, 1988, p. 428.

ACKNOWLEDGEMENTS. We thank Dr E. Desa, Director, National Institute of Oceanography, Goa, for the permission to publish this paper. We also thank Ritchie Sims, Tasha Black, Lorraine Hill and Vijay Khedekar for their assistance in various stages of the analysis. This paper was revised during J.N.P.'s stay under JSPS fellowship at Nagoya University, Nagoya, Japan. This is NIO contribution no. 3636.

Received 20 April 2000; revised accepted 22 December 2000

Stable isotopic studies of microbial carbonates from Talchir sediments of east-central India

Prosenjit Ghosh*, S. K. Bhattacharya*,‡ and A. Chakrabarti†

*Physical Research Laboratory, Navrangpura, Ahmedabad 380 009, India
†Department of Geology, Indian Institute of Technology, Kharagpur 721 302, India

Laminated microbial carbonate (LMC) bodies with micro-morphological features resembling algal stromatolites were found in two Talchir basins of east-central India. Samples of these bodies along with carbonate nodules obtained from the Talchir sediments were analysed geochemically. $d^{18}O$ and $d^{13}C$ values of the carbonate phase in the LMC range from 8.8 to 14.3‰ (w.r.t. SMOW) and –8.2 to –14.3‰ (w.r.t. PDB) respectively, indicating precipitation in freshwater environment. The carbon isotopic composition of carbonate free residual matter in the LMC ranges between –20.6 and –25.5‰. These values are similar to those of bacterial mats of modern lakes and confirm the biogenic origin of the LMC. The carbon to nitrogen ratio also matches with the composition of modern cyanobacterial matter. Presence of microbial mat on top of glacial debris suggests climatic amelioration subsequent to the sterile environment of Talchir glaciation.

UNUSUAL occurrence of calcareous body fossils resembling stromatolites or oncolites from Talchir sediments near Angul town in Orissa was first described by Pandya[1]. Subsequently, Mohanti and Das[2] inferred the presence of bacterial colony and fungal strands in a few of these objects based on SEM photographs. No further attempt has been made to characterize these bodies geochemically and confirm these earlier findings. Since the presence of stromatolite-type objects in Talchir sediments would be of great significance in the context of its environmental implications, we carried out isotopic characterization of these objects in the present work.

Talchir formation comprises terrigenous sequence of glacial boulders, varve sediments (siltstones) and shales deposited during the melting of Gondwana glaciers at the end of Permo-Carboniferous Glaciation. In peninsular India, these sediments were deposited in a few isolated basins along three major river valleys: Mahanadi, Damodar and Narmada. However, there has been some debate regarding the environment of deposition of Talchir sediments. Various sedimentary features like ripple mark, hummocky cross-stratification, etc. suggest that the sedimentation took place in a vast water body, but it was not clear if the glacial debris was deposited in a glacier-fed lake or a near-shore marine setting[3–5]. To resolve this controversy we carried out geochemical analysis of authigenically precipitated carbonate nodules which are frequently present in the siltstone bed of the Talchir Formation. The stable isotopic analyses of these nodular carbonates show that these deposits are formed in freshwater environment[6], possibly in lakes formed by melt-water from glaciers where waves and currents could operate[5]. During the course of these investigations we came across objects similar to those described by Pandya[1] in two Talchir exposures: Rai village (latitude: 23°23', longitude: 85°23') in Damodar Valley Basin and Nandirjhor Nala section (latitude: 20°48', longitude: 85°01') of Bedasar village near Angul town in Mahanadi Valley Basin (Figure 1). The present work is an attempt in deciphering the origin of these objects. The morphology of these objects is described below.

These laminated microbial carbonate (LMC) objects are botroidal in appearance and range in size from 30 to

†For correspondence. (e-mail: root@prl.ernet.in)